ELSEVIER

Biophysical Chemistry 91 (2001) 231–243

Biophysical Chemistry

www.elsevier.com/locate/bpc

Cloud-point temperatures for lysozyme in electrolyte solutions: effect of salt type, salt concentration and pH

J.J. Grigsby [a], H.W. Blanch [a,*], J.M. Prausnitz [a,b]

[a] *Chemical Engineering Department, University of California, Berkeley, CA 94720, USA*
[b] *Chemical Sciences Division, Lawerence Berkeley National Laboratory, Berkeley, CA 94720, USA*

Received 6 March 2001; received in revised form 4 May 2001; accepted 4 May 2001

Abstract

Liquid–liquid phase-separation data were obtained for aqueous saline solutions of hen egg-white lysozyme at a fixed protein concentration (87 g/l). The cloud-point temperature (CPT) was measured as a function of salt type and salt concentration to 3 M, at pH 4.0 and 7.0. Salts used included those from mono and divalent cations and anions. For the monovalent cations studied, as salt concentration increases, the CPT increases. For divalent cations, as salt concentration rises, a maximum in the CPT is observed and attributed to ion binding to the protein surface and subsequent water structuring. Trends for sulfate salts were dramatically different from those for other salts because sulfate ion is strongly hydrated and excluded from the lysozyme surface. For anions at fixed salt concentration, the CPT decreases with rising anion kosmotropic character. Comparison of CPTs for pH 4.0 and 7.0 revealed two trends. At low ionic strength for a given salt, differences in CPT can be explained in terms of repulsive electrostatic interactions between protein molecules, while at higher ionic strength, differences can be attributed to hydration forces. A model is proposed for the correlation and prediction of the CPT as a function of salt type and salt concentration. NaCl was chosen as a reference salt, and CPT deviations from that of NaCl were attributed to hydration forces. The Random Phase Approximation, in conjunction with a square-well potential, was used to calculate the strength of protein–protein interactions as a function of solution conditions for all salts studied.

Keywords: Cloud-point temperature; Lysozyme; Phase transition; Specific ion effect

* Corresponding author. Tel.: +1-510-642-4778; fax: +1-510-642-1387.
E-mail address: blanch@socrates.berkeley.edu (H.W. Blanch).

0301-4622/01/$ - see front matter
PII: S0301-4622(01)00173-9

1. Introduction

Association of biomacromolecules is essential for cellular structure and function; examples are provided by protein nucleic-acid binding and protein–protein binding [1]. However, protein association can also be detrimental to cellular function as, e.g. in the formation of cataracts and β-amyloid plaques [2,3]. Non-covalent forces including Coulombic, van der Waals and hydrophobic forces govern protein interactions. While these forces are understood on the level of small molecules, they remain obscure for complex macromolecules such as proteins.

Association of proteins provides the basis of common separation processes in industry and the laboratory, including salt-induced precipitation and crystallization. To achieve insight into how biomacromolecules interact, and to attain more efficient design and operation of protein separation processes, we require a better understanding of the effect of solution conditions on protein interactions. Salt-induced protein precipitation is often a first-step method for isolating protein molecules from an aqueous mixture of proteins or other biomacromolecules [4,5]. Although salt-induced precipitation is widely used, the forces leading to protein aggregation and subsequent precipitation are not well understood. Rules of thumb and empirical correlations are often used to adjust solution conditions to induce protein precipitation. A more efficient isolation method would be based on predicting the solution conditions (salt type and concentration, temperature, pH) that favor selective precipitation of a target protein.

Gast and Lekkerkerker [6,7] have shown that the range of attraction between colloid particles has a significant effect on the qualitative features of the phase diagram. When the range of attraction between particles is large compared to the size of the particles, the phase diagram resembles that of a simple fluid like argon. As the ratio of the range of attraction to the size of the particle decreases, the liquid–liquid critical point shifts to lower temperatures. If the range of attraction becomes sufficiently small (less than approx. 25% of the particle size), the liquid–liquid critical point becomes metastable. The work of Gast and Lekkerkerker is relevant to solutions of globular proteins whose attractive interactions are short-range. Rosenbaum and Zukowski [8,9] have shown that protein crystallization is strongly enhanced in a narrow region of the protein phase-diagram. Protein crystals were shown to form in a narrow window near the metastable critical point.

Frenkel et al. reported numerical simulations of protein-crystal nucleation for globular proteins with short-range attractive interactions [10,11]. The free-energy barrier for crystal nucleation was strongly reduced near the metastable critical point, leading to increased rates of crystal nucleation. Because the location of the metastable critical point is a function of solvent conditions, their simulations suggest a systematic approach to promote protein crystallization.

A metastable liquid–liquid region for protein solutions has been observed experimentally for γ-crystallin [12,13] and for lysozyme [14–16]. Broide et al. measured the cloud-point temperature (CPT) and the crystallization temperature (CT) for lysozyme as a function of salt type and concentration at pH 7.8. The CPT provides a measure of the net attractive interactions between protein molecules. The higher the CPT, the greater the net attractive interactions. Broide et al. found that the CPT was typically 15–45°C below the crystallization temperature.

To further examine the role of salt type on interprotein interactions, we report CPT measurements for hen egg-white lysozyme at pH 4.0 and 7.0 for a fixed protein concentration of 87 g/l as a function of both salt type and salt concentration. Anions studied were Cl^-, NO_3^- and SO_4^{2-}. Cations studied were Na^+, K^+, NH_4^+, Ca^{2+} and Mg^{2+}. The effect of salt type on CPT is related qualitatively to the kosmotropic or chaotropic nature of the salt and through protein-ion binding. A phenomenological potential of mean force (PMF) model is proposed to represent the observed specific nature of the salt–protein interaction and the effect of pH.

2. Materials and methods

2.1. Protein and salt-solution preparation

Lysozyme was from Boehringer Mannheim (Germany). Since gel electrophoresis indicated less than 1% contamination by other proteins, no further purification was performed. Reagent-grade NaCl, KCl, NH_4Cl, $MgCl_2$, $CaCl_2$, $NaNO_3$, NH_4NO_3, $Mg(NO_3)_2$, KNO_3, $Ca(NO_3)_2$, Na_2SO_4, K_2SO_4, $(NH_4)_2SO_4$ and $MgSO_4$ were from Fischer Scientific (Pittsburgh, PA). Tris buffer and sodium azide were from Sigma (St. Louis, MO). Deionized water was obtained from a Barnsteaed-Nanopure II filtration unit.

A 4-l stock solution of 20-mM Tris buffer was prepared. Lysozyme was dissolved in a small volume of the stock solution. Although gel electrophoresis showed minimal protein contamination, small amounts of salts in the lyophilized lysozyme may influence protein–protein interactions. Therefore, the protein solution was dialyzed against the buffer solution for 24 h at 4°C to minimize the amount of salt contamination. Dialysis tubing with molecular-weight cut-off 6000–8000 Da was from Spectrum Medical Industries (Los Angeles, CA). After dialysis, sodium azide was added to the protein solution at a concentration of 2 mM to prevent bacterial growth. The pH of the solution was adjusted with concentrated HCl or NaOH.

The lysozyme solution was concentrated using an Amicon Ultrafiltration Unit with 3000 Da cut-off membranes (Beverly, MA). After the ultrafiltration process, the pH of the protein solution was again adjusted with HCl or NaOH. The protein solution was centrifuged at 20 000 rpm for 20 min to remove any aggregates present after ultrafiltration.

Lysozyme concentration was determined by measuring absorbance at 280 nm and 25°C using a Beckman DU-6 spectrophotometer, employing an extinction coefficient of 2.635 l/g-cm [17], with lysozyme dilutions of 1:500 and 1:1000 in deionized water. The calculated lysozyme concentrations from the two dilution sets were averaged with a standard deviation less than 0.8 g/l. The lysozyme solution was kept at 4°C. No visible aggregates were observed in the protein solution for the duration of the cloud-point temperature measurements. The pH of the solution was checked periodically and remained within 0.2 pH units.

A stock salt solution was prepared by dissolving the salt of interest in 20-mM Tris buffer. A range of salt-solution concentrations was prepared by dilution of the stock solution with deionized water containing 20-mM Tris buffer. Any volume change upon mixing was assumed to be negligible. The pH of each solution was checked after mixing.

2.2. Cloud-point temperature measurements

The CPT detection system contained an Innova-90 argon-ion laser (Coherent inc., Santa Clara, CA) tuned to a wavelength of 488 nm, a BI-240SM multi-angle goniometer, a BI-EMI-9865 photomultiplier and a BI-9000 digital autocorrelator, which measures the amount of scattered light in real time. Light-scattering measurements were taken at a 90° scattering angle. Constant temperature was achieved with a VWR Model 1160 recirculating water-ethanol bath.

The volumes of protein solution and salt solution needed to achieve a lysozyme concentration of 87 g/l upon mixing were calculated. The final salt concentration was calculated from the initial salt concentration and from the final volume of the aqueous protein–salt solution. The protein and salt solutions were mixed in precision-ground pyrex NMR tubes with 12-mm O.D., 0.5-mm wall thickness (Wilmad Glass, Buena, NJ) and sealed with a plastic cap to prevent water loss during CPT measurements.

The sample tube was placed in the CPT detection system and allowed to thermally equilibrate for 30 min. For an initial estimate of the CPT, the temperature of the sample was reduced at 2°C/min to find the temperature range for the onset of cloud formation. Close to the clouding-onset temperature there is a dramatic increase in the amount of scattering light due to differences in the refractive indices of the emerging protein-rich and protein-poor phases. Once the temperature range for the onset of clouding was es-

tablished within 0.5°C, the temperature of the sample was reduced in increments of 0.1°C. For each increment, the sample was allowed to equilibrate for 15 min. The onset-clouding temperature, T_{cloud}, was noted. Next, the temperature of the sample was increased slowly (0.2°C/min) until the sample became clear. Once the temperature range for the onset of declouding was established within 0.5°C, the temperature of the sample was increased in increments of 0.1°C again allowing 15 min for equilibration. The temperature where the sample became clear, T_{clear}, was noted. The difference between T_{cloud} and T_{clear} was in the range of 1.0 to 3.0°C, depending on the salt type and salt concentration. The reported CPT is taken to be the average of T_{cloud} and T_{clear}. The liquid–liquid phase transition for most salts was quite distinct over a narrow temperature range. The CPT measurements were reproducible within 0.2°C.

3. Results

Figs. 1 through 5 show experimental cloud-point temperatures. Tables of CPT are available elsewhere [18]. Figs. 1 and 2 show the effects of the cation on CPT for pH 4.0 and 7.0, respectively. Figs. 3 and 4 show the effects of the anion on CPT for pH 4.0 and 7.0, respectively. Fig. 5 shows the effect of pH on CPT for representative salts.

The CPT results depend strongly on the specific nature of the ions. Kosmotropic ions bind adjacent water molecules more strongly than water binds itself. When a kosmotropic ion is introduced into water, the entropy of the system decreases due to increased water structuring around the ion. In contrast, chaotropes bind adjacent water molecules less strongly than water binds itself. When a chaotrope is introduced into water, the entropy of the system increases because the water structuring around the ion is less than that in salt-free water. This classification is related to the size and charge of the ion. Ions with high charge density such as Mg^{2+}, Ca^{2+} and SO_4^{2-} are highly kosmotropic. Ions with low charge density such as K^+, NH_4^+ and NO_3^- are chaotropic, NO_3^- is strongly chaotropic. Na^+ is weakly kosmotropic and Cl^- is weakly chaotropic [19]. We discuss the CPT results in terms of the chaotropic or kosmotropic nature of the anions and cations.

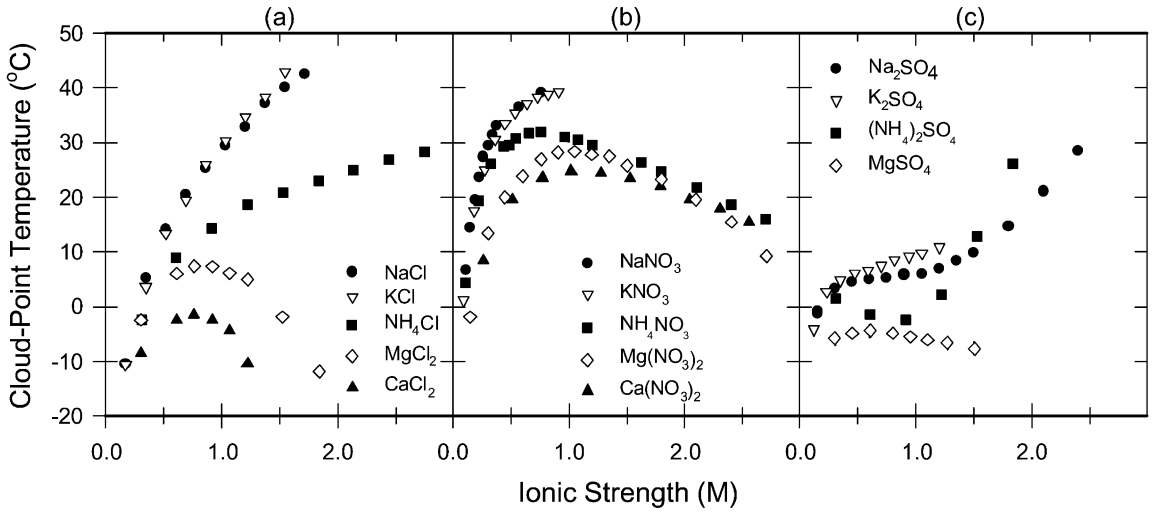

Fig. 1. Effect of cations on the CPT for lysozyme (87 g/l) at pH 7.0 for (a) Cl^-, (b) NO_3^- and (c) SO_4^{2-} aqueous salt solutions. For different salts, as ionic strength increases the difference in CPT increases, indicating the specific nature of the ions is more important at higher salt concentration. A maximum in the CPT is observed for divalent cationic salts.

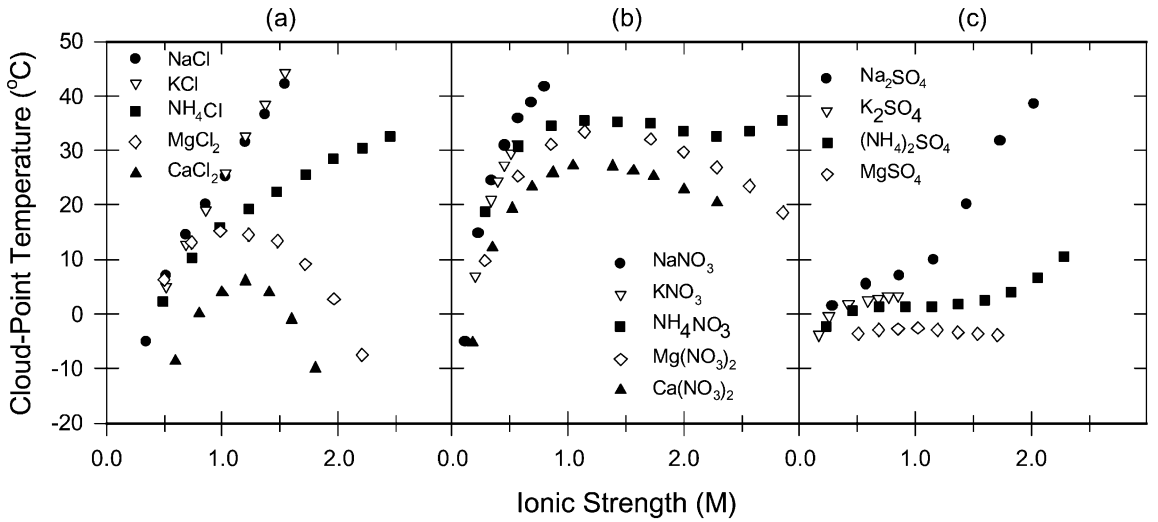

Fig. 2. Effect of cations on the CPT for lysozyme (87 g/l) at pH 4.0 for (a) Cl^-, (b) NO_3^- and (c) SO_4^{2-} aqueous salt solutions. The trends for pH 4.0 are similar to pH 7.0.

3.1. Effect of cations

Figs. 1 and 2 compare CPT data for various cations at pH 7.0 and 4.0, respectively. The trends are similar at both pHs. For different salts, as ionic strength decreases, the difference in CPT declines, indicating that the specific nature of the ion is less important at an ionic strength less than 0.3 M. CPT measurements could not be obtained at lower salt concentrations because the solution

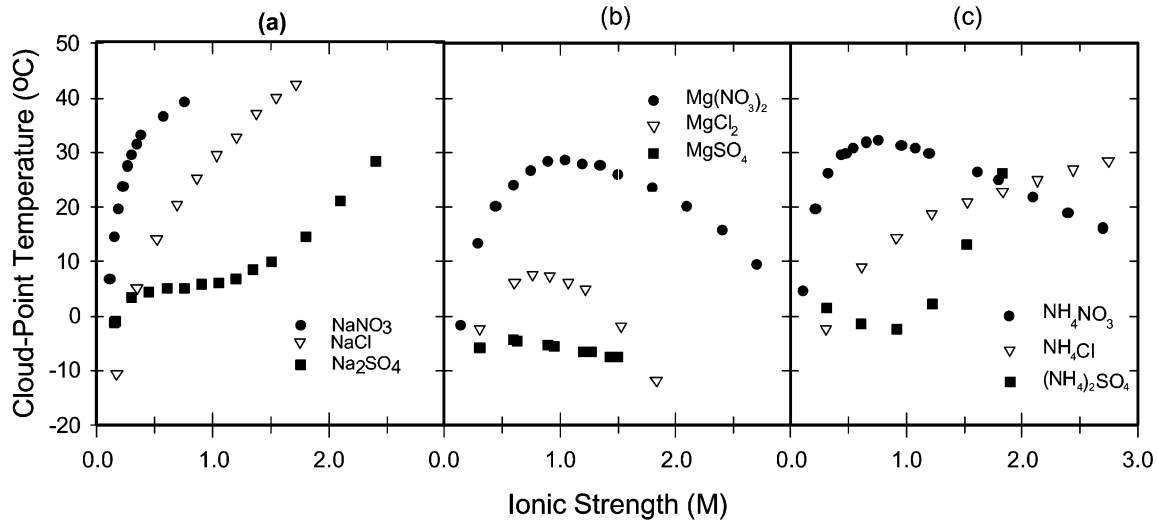

Fig. 3. Effect of anions on the CPT for lysozyme (87 g/l) at pH 7.0 for (a) Na^+, (b) Mg^{2+} and (c) NH_4^+ aqueous salt solutions. The CPT decreases as the anion becomes more kosmotropic at a fixed salt concentration. While potassium and calcium salts are not included, they follow the same trends as the sodium and magnesium salts, respectively.

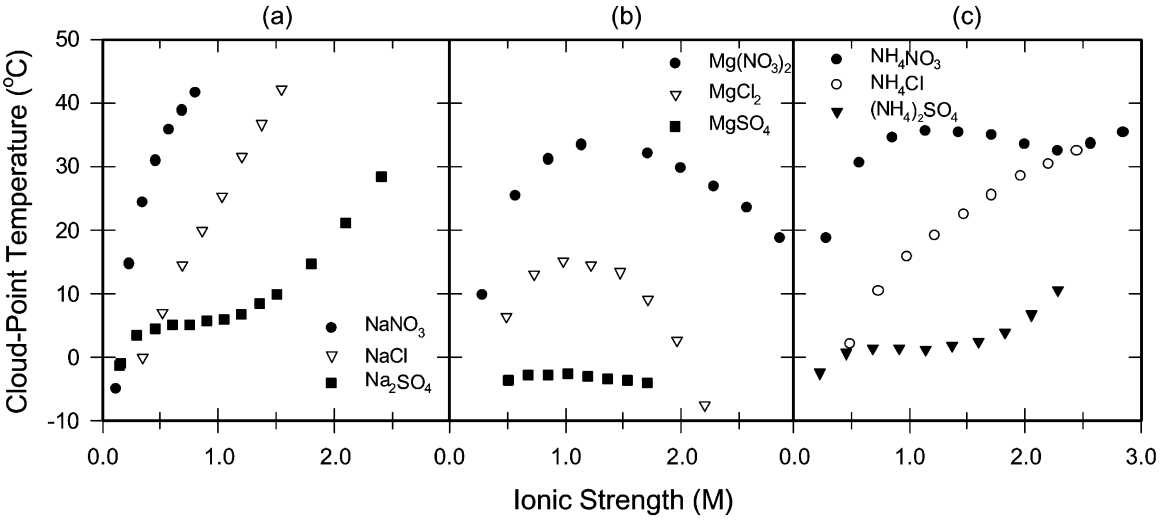

Fig. 4. Effect of anions on the CPT for lysozyme (87 g/l) at pH 4.0 for (a) Na^+, (b) Mg^{2+} and (c) NH_4^+ aqueous salt solutions. Trends are similar to pH 7.0. The trends for potassium and calcium salts are similar to the sodium and magnesium salts, respectively.

formed ice crystals before a liquid–liquid phase separation was observed. The difference in CPT becomes dramatic for different salt types above ionic strength 0.3 M.

Fig. 1a and Fig. 2a show CPT data for several cations of chloride salts at pH 7.0 and 4.0, respectively. For NaCl and KCl, the CPT shows similar values with increasing ionic strength. CPT increases less sharply with ionic strength for NH_4Cl than for NaCl or KCl. For the divalent salts

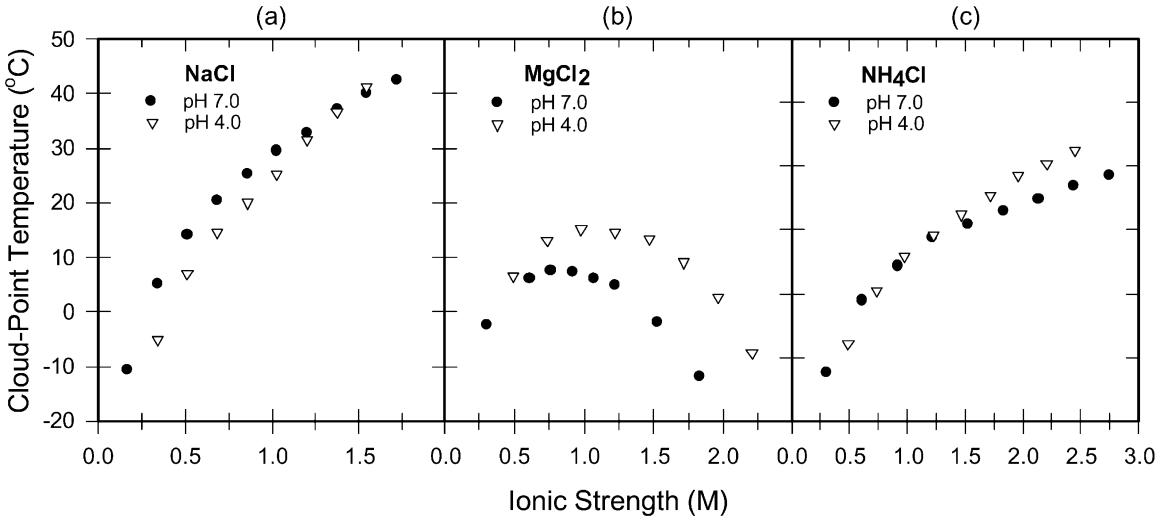

Fig. 5. Effect of pH on the CPT for lysozyme (87 g/l) for (a) NaCl, (b) $MgCl_2$ and (c) NH_4Cl aqueous salt solutions. For NaCl, as salt concentration increases, the difference in CPT decreases due to charge screening. For $MgCl_2$, as salt concentration increases, the difference in CPT increases. Greater Mg^{2+} binding to the lysozyme surface at pH 7.0 leads to a greater hydration force and hence a lower CPT. The trend for NH_4Cl is a combination of charge screening and hydration force effects.

$MgCl_2$ and $CaCl_2$, a maximum is observed in the CPT at ionic strength 0.8 M at pH 7.0 and at 1.0 M at pH 4.0. The maximum is due to binding of the highly kosmotropic ions Mg^{2+} and Ca^{2+} to the protein. Ion binding to the protein surface and subsequent structuring of water around the ion produces a repulsive barrier, which is the hydration force.

Hydration forces may be observed from surface-force measurements. At very short separation distances (less than 2 nm), charged bilayers adsorbed on mica surfaces are more repulsive than expected due to steric hydration interactions between the hydrophilic headgroups that characterize the surface [20]. Pashley has shown that the interaction between bare mica surfaces in concentrated electrolyte solutions gives rise to a repulsive hydration force that follows from binding of hydrated cations to the negatively charged surfaces [21–25]. The magnitude of this force is related to the energy needed to dehydrate the bound cations, which retain some of their water of hydration upon binding. The strength and range of hydration forces increases with the hydration number of the cation. When a kosmotropic ion binds to an oppositely charged residue on the protein surface, the extent of water structuring at the protein surface increases. Chaotropes do not interact strongly with oppositely charged residues on the protein surface due to their low charge density but tend to disrupt the structure of water in the bulk solution.

For two protein molecules to approach each other to form a second, more-dense phase, the water structure surrounding the protein surface must be broken. As the concentration of the divalent cation increases, the extent of ion binding and subsequent water structuring at the surface increases. The repulsive hydration force grows with rising salt concentration. A second more-dense liquid phase becomes increasingly energetically unfavorable at higher salt concentrations due to the rise in the repulsive hydration force. Therefore, the CPT falls at higher salt concentrations.

The trends in Fig. 1b and Fig. 2b for nitrate salts are similar to those for chloride salts. However, at lower salt concentrations, CPT increases more dramatically for nitrate salts. CPT measurements could not be taken at higher salt concentrations for $NaNO_3$ and KNO_3 due to the appearance of irreversible aggregates at temperatures above 45°C, possibly because of thermal protein denaturation.

As indicated in Fig. 1c and Fig. 2c, for the sulfate series, the CPT trends are significantly different from those for chloride and nitrate salts. CPT measurements could not be taken at high K_2SO_4 or $CaSO_4$ concentrations due to low salt solubility. It is known that the lyotropic series for lysozyme is reversed relative to most proteins [26]. The sulfate ion, a good salting-in ion for lysozyme, has been shown to be preferentially excluded at the lysozyme surface [27,28]. When compared to chloride and nitrate salts, the CPT increases at a much slower rate as salt concentration rises. Above ionic strength 1.0 M, the CPT begins to rise dramatically for Na_2SO_4 and $(NH_4)_2SO_4$. This rise is due to a competition for water to hydrate the protein surface or the sulfate ion. The sulfate ion is highly kosmotropic and therefore, interacts strongly with water molecules. At low salt concentrations, the solution contains a sufficient number of water molecules to hydrate both the protein surface and the sulfate ions. At higher salt concentrations, more water molecules are needed to hydrate the increasing number of sulfate ions. The formation of a second more-dense protein phase provides more free water molecules to hydrate the sulfate ions because of the lower number of water molecules needed to hydrate the protein molecules in the dense phase. A slight maximum in CPT is observed for $MgSO_4$, but the CPT does not change significantly over the entire salt concentration range. The effects of the magnesium and sulfate ions appear to cancel each other at higher salt concentrations. Magnesium ion preferentially interacts at the protein surface leading to a repulsive hydration force while the sulfate ion dehydrates the protein surface leading to an attractive force.

3.2. Effect of anions

Figs. 3 and 4 compare the effect of anions on CPT at pH 7.0 and 4.0, respectively. While results

for potassium and calcium salts are not shown, they follow the same trends as those for the sodium and magnesium salts, respectively. In all plots, as the anion becomes more kosmotropic, the CPT decreases at a specific salt concentration. This specificity follows from the extent of water structuring in the system. Sulfate is highly kosmotropic, chloride marginally chaotropic and nitrate very chaotropic. There is a greater solution structure for sulfate salts compared to nitrate salts. The greater the solution structure, the greater is the repulsive hydration force and, hence this leads to a lower CPT.

3.3. The effect of pH

Fig. 5 compares the CPT at pH 4.0 and pH 7.0 for NaCl, $MgCl_2$ and NH_4Cl. While results for potassium and calcium salts are not shown, the trends for these salts are the same as those for sodium and magnesium salts, respectively. In addition, the nitrate salts follow the same trends as the chloride salts.

Fig. 5a compares results for NaCl at pH 4.0 and 7.0. As the concentration of salt rises, the difference between the CPT between the two pHs decreases and disappears at ionic strength above 1.3 M. This decrease and disappearance follows from salt screening of the charge–charge repulsion between the protein molecules. The net charge of lysozyme is $+11$ at pH 4.0 and $+8$ at pH 7.0. At a fixed salt concentration below 1.3 M, the net attractive interactions measured by the CPT are less at pH 4.0 due to greater charge–charge repulsion at this pH. As the concentration of salt increases, the repulsive charge–charge interaction between protein vanishes because it is screened by the salt ions. This trend can be seen in all CPT data at low salt concentrations. The concentration of salt for complete screening is much higher than that predicted from DLVO theory (approx. 0.1 M). The concentrations of protein and salt are far from the dilute region and therefore, the DLVO mean-field approximation is no longer valid. The concentration where charge–charge screening is complete depends on the nature of the ions.

Fig. 5b compares the effect of pH on CPT for $MgCl_2$. Above the salt concentration where charge screening occurs, the CPT data begin to diverge. The difference between the CPT at pH 4.0 and 7.0 increases with salt concentration. The CPT at pH 4.0 is always greater than that at pH 7.0. This difference follows from Mg^{2+} binding to the protein surface. Magnesium and calcium are kosmotropic ions that have been shown to bind to the surface of lysozyme [27]. The number of ions that can bind to that surface depends on the charge of the protein. Because the net positive charge on the lysozyme molecule is less at pH 7.0, more cations can bind to the surface at pH 7.0 than at pH 4.0. Binding of kosmotropes to the surface of a protein produces more water structuring at the protein surface, leading to a hydration barrier to protein aggregation. With rising salt concentration, the extent of this hydration barrier increases, as indicated by the CPT data. Although ammonium is not a kosmotropic ion, the CPT trends suggest that this ion is binding to the protein surface.

The effect of pH on the CPT for sulfate salts differs from the trends seen in the chloride and nitrate salts. Significant differences in the CPT appear above 1 M due to the greater competition for binding water to the protein surface and to the sulfate ion. The trends for K_2SO_4 and $CaSO_4$ are similar to those for Na_2SO_4 and $MgSO_4$, respectively.

3.4. Potential of mean force for protein–protein interactions

The Derjaguin–Landau–Verwey–Overbeek (DLVO) theory has been used extensively to account for protein–protein interactions in dilute solutions of protein and salt. The DLVO theory accounts for repulsive Coulombic interactions due to protein-surface charge and attractive interactions arising from van der Waals forces. The Coulombic term is derived from a mean-field approximation and therefore, does not take into account the discrete nature of the salt ions. In DLVO theory, the extent of charge screening between protein molecules is a function of ionic strength only, and quickly approaches zero at ionic strengths above 0.1 M. The attractive van

der Waals forces between protein molecules is believed to be essentially independent of ionic strength because fluctuations in the positions of the electrons of the protein leading to dispersion forces are on a time scale much shorter than that of ion rearrangement.

DLVO theory has been successful in explaining solution behavior of dilute protein and salt solution, however, it cannot account for protein precipitation, crystallization and liquid–liquid phase separation which occurs in concentrated salt solutions. In this study, we are interested in the behavior of specific ions, and consider ion size, charge, ability to bind to the protein surface and interactions of the ions with water molecules.

In an attempt to correlate and provide a means of predicting the CPT data, we employ a square-well potential of mean force $W(r)$ to describe the interactions of two lysozyme molecules in an electrolyte solution:

$$W(r) = \begin{cases} \infty & r < \sigma \\ -\varepsilon & \sigma \le r \le \sigma + \delta \\ 0 & \sigma + \delta < r \end{cases} \quad (1)$$

where r is the center-to-center distance between two protein molecules, σ is the protein diameter, ε is the depth of the square well and δ is the width of the square well. The width of the square well is assumed to be 20% of the protein diameter as suggested by Frenkel [10,11], who showed that when the range of attraction between protein molecules is less than 25% of the protein diameter, a metastable liquid–liquid region appears. We set $\sigma = 34.4$ Å, the hard sphere diameter of a lysozyme molecule determined from X-ray crystallography. Hence, $\delta = (0.2)\ (34.4\ \text{A}) = 6.9$ Å.

To describe liquid–liquid equilibria, we use the Random Phase Approximation (RPA) to generate expressions for the pressure and chemical potential [29]. The equation for pressure P is:

$$\frac{P}{\rho kT} = \left(\frac{P}{\rho kT}\right)_{\text{ref}} + \frac{\rho U}{2kT} \quad (2)$$

where, ρ is the protein number density, k is Boltzmann's constant, T is the CPT, and U is the perturbation energy per unit density. The reference pressure is that of a hard-sphere system and is given by the Carnahan–Starling expression:

$$\left(\frac{P}{\rho kT}\right)_{\text{ref}} = \frac{1 + \eta + \eta^2 - \eta^3}{(1-\eta)^3} \quad (3)$$

where $\eta = (\pi\rho/6)\sigma^3$ is the protein packing fraction. The perturbation term accounts for interactions between protein molecules including charge–charge, van der Waals and hydration interactions. The perturbation energy per unit density is related to the potential of mean force as given in Eq. (4):

$$U = 4\pi \int W(r)\, r^2\, \mathrm{d}r \quad (4)$$

The chemical potential μ is:

$$\frac{\mu - \mu'}{kT} = \frac{\eta(8 - 9\eta + 3\eta^2)}{(1-\eta)^3} + \frac{\rho U}{kT} + \ln\rho \quad (5)$$

where μ' is the reference chemical potential that is the same in both liquid phases.

For two phases α and β, the following conditions must be met:

$$\mu^\alpha = \mu^\beta, \quad (6)$$

$$P^\alpha = P^\beta. \quad (7)$$

Because at the onset of clouding, the volume of the dense phase that forms is negligibly small compared to the total volume, the protein concentration in the supernatant phase is equal to the initial protein concentration. There are two unknowns in Eqs. (6) and (7), ε and the protein packing fraction in the dense phase, η^β. Input parameters are the known initial protein packing fraction, η^α and the measured CPT.

Toward interpreting the significance of the interprotein energy parameter ε, we define a reference state. For comparison of salts, NaCl was chosen as a 'reference salt' because Na^+ is marginally kosmotropic and Cl^- is marginally chaotropic. The difference between the entropy of pure water and the entropy of water near Na^+ or Cl^- is nearly zero [30,31]. Although Cl^- has

been shown to bind to lysozyme [32–34], any subsequent solution restructuring at the ion-binding site can be considered to be minimal compared to highly kosmotropic or chaotropic ions such as Mg^{2+} or NO_3^-. Therefore, NaCl was selected as an appropriate reference salt. Using CPT data for lysozyme solution containing NaCl, ε_{NaCl} was calculated as a function of salt concentration at pH 4.0 and 7.0.

At a fixed ionic strength, deviations of the CPT for a salt relative to that for NaCl were attributed to specific ion interactions with lysozyme. For all salts except NaCl, a change in the square-well potential was introduced to account for these specific ion effects and is given by:

$$W(r,I) = -\left[\varepsilon_{NaCl}(I) + \varepsilon_{sp}(I)\right] \quad (8)$$

where I is the ionic strength. To calculate $\varepsilon_{sp}(I)$ and η^{β}, we use as input the calculated $\varepsilon_{NaCl}(I)$, the known initial protein packing fraction η^{α} and the measured CPT of the salt.

3.5. Parameter estimation

The depth of the square well was calculated for the reference salt NaCl as a function of ionic strength for pH 4.0 and 7.0 at the CPT. Table 1 shows ε_{NaCl} as a function of ionic strength.

Deviations of the CPT from the reference are due to specific ion effects, including hydration forces and water structuring of the solution. To calculate the corresponding $\varepsilon_{sp}(I)$, the equations in Table 1 were used in conjunction with CPT data for the other salts in Eq. (8). When needed, values for ε_{NaCl} were extrapolated beyond those obtained from measured CPTs for NaCl, using the equations in Table 1.

Table 2 gives equations for $\varepsilon_{sp}(I)/kT$ at pH 4.0 and 7.0 where T is the CPT. For monovalent salts, $\varepsilon_{sp}(I)/kT$ is linear with ionic strength and for divalent cationic salts, $\varepsilon_{sp}(I)/kT$ is linear with the square of ionic strength. For sulfate salts $\varepsilon_{sp}(I)/kT$ is parabolic in ionic strength.

For salts containing either Na^+ or Cl^-, the ε_{sp}/kT results in Table 2 reflect effects due to the appropriate counterion. For example, the

Table 1
Relationship between the depth of the square well, ε_{NaCl}, and ionic strength, I (M), for lysozyme (87 g/l) in NaCl solutions at pH 4.0 and 7.0 at the CPT. ε_{NaCl} was made dimensionless through division by kT where T was chosen to be 298 K

pH	Fitted equation
4.0	$\varepsilon_{NaCl}/kT = 0.38 \ln(I) + 3.78$
7.0	$\varepsilon_{NaCl}/kT = 0.29 \ln(I) + 3.82$

ε_{sp}/kT values for $MgCl_2$ are attributed to the Mg^{2+} ion only. Combinations for ε_{sp}/kT for ions other than Na^+ or Cl^- can be used to predict the CPT. This model is based on a fixed protein concentration of 87 g/l. Further CPT data as a function of protein concentration is needed to assess whether ε_{sp}/kT is dependent on protein concentration.

Combinations of ε_{sp}/kT for all ions were performed and compared to ε_{sp}/kT values obtained through experiment and subsequent calculations. Fig. 6 shows representative results for combinations of (a) monovalent ions, (b) divalent cation and NO_3^- and (c) monovalent cation with SO_4^{2-}. Addition of ε_{sp}/kT for monovalent ions showed good agreement to experimentally measured CPT data for all ions. For example, ε_{sp}/kT for NH_4NO_3 was predicted by addition of ε_{sp}/kT for NH_4Cl and $NaNO_3$. Since NaCl is the reference salt, the contribution to ε_{sp}/kT by NH_4Cl is solely due to NH_4^+ since the contribution by Cl^- is zero. Similarly, the contribution to ε_{sp}/kT by $NaNO_3$ is solely due to NO_3^- since the contribution by Na^+ is zero. Simple addition of energetic parameters did not show good agreement for divalent cationic salts. Instead, the average of ε_{sp}/kT for the divalent cation and monovalent anion did show very good agreement, even at high ionic strength for both magnesium and calcium salts. For example, ε_{sp}/kT for $Mg(NO_3)_2$ was computed by adding the equations from Table 2 for $MgCl_2$ and $NaNO_3$ and subsequently taking the average of the result. One explanation for why the average gave good results and not the simple addition is due to the nature of the ions. Mg^{2+} and Ca^{2+} are highly kosmotropic and increase the extent of solution structure while the

Table 2
Energy parameters ε_{sp}/kT as a function of ionic strength (I) and salt type[a]

	Salt	$\varepsilon_{sp}/kT=(mI+b)$ pH 4.0		$\varepsilon_{sp}/kT=(mI+b)$ pH 7.0	
		m	b	m	b
Monovalent	$NaNO_3$	−0.34	0.55	−0.29	0.42
	KCl	0.08	−0.08	0.03	−0.02
	KNO_3	−0.34	0.47	−0.28	0.40
	NH_4Cl	−0.11	−0.02	−0.08	−0.08
	NH_4NO_3	−0.26	0.39	−0.31	0.36
		$\varepsilon_{sp}/kT=(mI^2+b)$ pH 4.0		$\varepsilon_{sp}/kT=(mI^2+b)$ pH 7.0	
		m	b	m	b
Divalent cation	$MgCl_2$	−0.17	0.04	−0.15	−0.15
	$Mg(NO_3)_2$	−0.09	0.20	−0.09	0.09
	$CaCl_2$	−0.18	−0.14	−0.33	−0.14
	$Ca(NO3)_2$	−0.11	0.14	−0.08	0.01
		$\varepsilon_{sp}/kT=(gI^2+mI+b)$ pH 4.0			$\varepsilon_{sp}/kT=(gI^2+mI+b)$ pH 7.0		
		g	m	b	g	m	b
Divalent anion	Na_2SO_4	0.39	−1.02	0.41	0.26	0.82	0.25
	K_2SO_4	0.81	−1.65	0.58	0.43	−1.01	0.31
	$(NH_4)_2SO_4$	0.26	−1.00	0.40	0.55	−1.28	0.32
	$MgSO_4$	0.17	−0.81	0.23	0.20	−0.80	0.11

[a] I is in mol/l and T is the CPT at a specific I. These parameters represent the deviations from ε_{NaCl} due to specific ion effects. ε_{sp}/kT is linear with I for monovalent salts, and quadratic for divalent cationic salts. Data for the sulfate series were fit to a second-order polynomial. The equations in Table 1 and Table 2 can be used to predict the CPT of lysozyme for numerous salts over a wide concentration range.

highly chaotropic ion NO_3^- breaks up the solution structure. The competing processes of increasing and decreasing the extent of water structure lead to an average effect. The proposed potential of mean force model predicts good results for K_2SO_4 for all salt concentrations and for $(NH_4)_2SO_4$ below 1 M through addition of ε_{sp}/kT.

4. Conclusion

Experimental cloud-point data show that classical DLVO theory is inadequate at high lysozyme and salt concentrations. To interpret the data, a square-well potential of mean force was proposed to account for specific effects of different ions. The width of the square-well was fixed at 20% of the protein diameter with NaCl as a reference salt. The depth of the square well ε_{sp} was calculated for other salts relative to NaCl. Plots of ε_{sp}/kT as a function of ionic strength show that for monovalent salts, the trends are linear in ionic strength, whereas the trends for divalent cationic salts show a quadratic dependence. Combinations of the regressed energy parameters for ions were used to predict the CPT for a particular salt. Predicted and measured results show good agreement for monovalent and cationic salts over the entire salt concentration range and to 1 M for sulfate salts.

Acknowledgements

This work was supported by the National Sci-

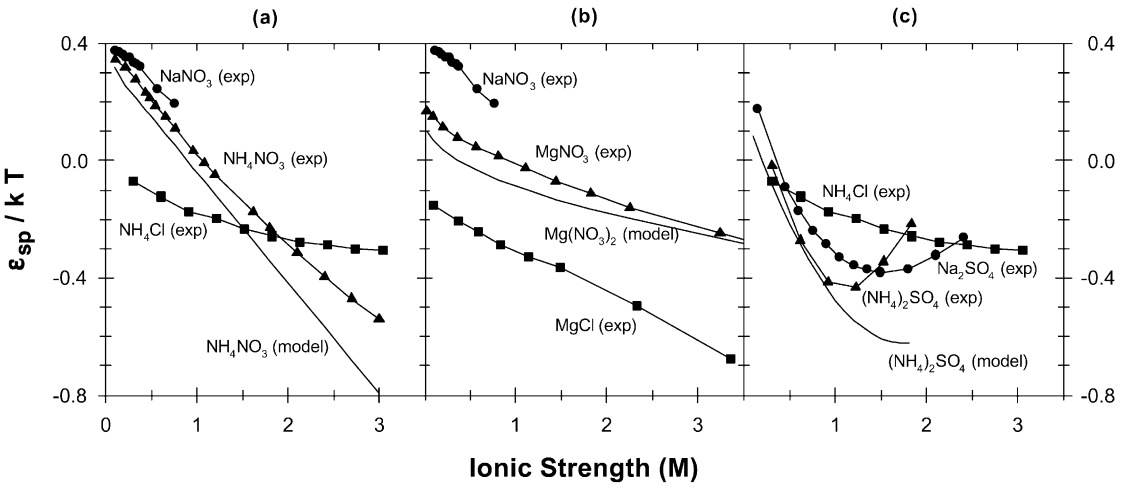

Fig. 6. Representative plots of combinations of ε_{sp}/kT for (a) monovalent ions, (b) divalent cations and NO_3^- and (c) monovalent cations with SO_4^{2-}. NaCl was chosen as a reference salt, and therefore, Na^+ and Cl^- do not contribute to ε_{sp}/kT of the appropriate counterion. The solid line (no symbols) represents ε_{sp}/kT calculated from the model (a) Shows that addition of ε_{sp}/kT values gives good results. (b) Shows the average of ε_{sp}/kT gives good results (Mg^{2+} is a solution structure former and NO_3^- is a structure breaker). (c) Shows the addition of ε_{sp}/kT gives good agreement up to 1 M.

ence Foundation CT59530793 and by the Director, Office of Science, Office of Basic Energy Sciences, Chemical Sciences Division of the US Department of Energy under Contract Number DE-AC0376SF0009.

References

[1] W.P. Jenck, Binding-energy, specificity and enzymatic catalysis, circe effect, Adv. Enzymol. RAMB 43 (1975) 219–410.
[2] T.S. Burkoth, T.L.S. Benzinger, V. Urban et al., Structure of the beta-amyloid(10-35) fibril, J. Am. Chem. Soc. 122 (2000) 7883–7889.
[3] B. Drouet, M. Pincon-Raymond, J. Chambaz, T. Pillot, Molecular basis of Alzheimer's disease, Cell. Mol. Life Sci. 57 (2000) 705–715.
[4] F. Rothstein, Protein Purification Process Engineering, Dekker, New York, 1994.
[5] R.K. Scopes, Protein Purification: Principles and Practice, Springer-Verlang, New York, 1994.
[6] A.P. Gast, C.K. Hall, W.B. Russel, Polymer-induced phase separations in non-aqueous colloidal suspensions, J. Colloid Interf. Sci. 96 (1983) 251–267.
[7] H.N.W. Lekkerkerker, W.C.K. Poon, P.N. Pusey, A. Stroobants, P.B. Warren, Phase-behavior of colloid plus polymer mixtures, Europhys. Lett. 20 (1992) 559–564.
[8] D. Rosenbaum, P.C. Zamora, C.F. Zukoski, Phase-behavior of small attractive colloidal particles, Phys. Rev. Lett. 76 (1996) 150–153.
[9] D.F. Rosenbaum, C.F. Zukoski, Protein interactions and crystallization, J. Cryst. Growth 169 (1996) 752–758.
[10] P.R. ten Wolde, D. Frenkel, Enhancement of protein crystal nucleation by critical density fluctuations, Science 277 (1997) 1975–1978.
[11] P.R. ten Wolde, D. Frenkel, Enhanced protein crystallization around the metastable critical point, Theor. Chem. Acc. 101 (1999) 205–208.
[12] M.L. Broide, C.R. Berland, J. Pande, O.O. Ogun, G.B. Benedek, Binary-liquid phase-separation of lens protein solutions, Proc. Natl. Acad. Sci. USA 88 (1991) 5660–5664.
[13] D.W. Liu, A. Lomakin, G.M. Thurston et al., Phase-separation in multicomponent aqueous-protein solutions, J. Phys. Chem. 99 (1995) 454–461.
[14] V.G. Taratuta, H. Holschbach, G.M. Thurston, D. Blankschtein, G.B. Benedek, Liquid-liquid phase separation of aqueous lysozyme solutions, effects of pH and salt identity, J. Phys. Chem. 94 (1990) 2140–2144.
[15] M.L. Broide, T.M. Tominc, M.D. Saxowsky, Using phase transitions to investigate the effect of salts on protein interactions, Phys. Rev. E 53 (1996) 6325–6335.
[16] M. Muschol, F. Rosenberger, Liquid–liquid phase separation in supersaturated lysozyme solutions and associated precipitate formation/crystallization, J. Chem. Phys. 107 (1997) 1953–1962.
[17] A.J. Sophianopoulos, K.E. Van Holde, Physical studies of muramidase (lysozyme) II. pH-dependent dimerization, J. Biol. Chem. 230 (1964) 2516–2524.
[18] J.J. Grigsby, Ph.D. Thesis, University of California, Berkeley, 2001.

[19] K.D. Collins, Charge density-dependent strength of hydration and biological structure, Biophys. J. 72 (1997) 65–76.
[20] A.C. Cowley, N.L Fuller, R.P. Rand, V.A. Paarsegian, V.A. Rsegian, Measurement of repulsive forces between charged phospholipid bilayers, Biochemistry 17 (1978) 3163–3168.
[21] R.M. Pashley, DLVO and hydration forces between mica surfaces in Li^+, Na^+, K^+, and Cs^+ electrolyte-solutions: a correlation of double-layer and hydration forces with surface cation-exchange properties, J. Colloid Interf. Sci. 83 (1981) 531–546.
[22] R.M. Pashley, Hydration forces between mica surfaces in aqueous-electrolyte solutions, J. Colloid Interf. Sci. 80 (1981) 153–162.
[23] R.M. Pashley, Hydration forces between mica surfaces in electrolyte-solutions, Adv. Colloid Interf. Sci. 16 (1982) 57–62.
[24] R.M. Pashley, J.N. Israelachvili, DLVO and hydration forces between mica surfaces in Mg^{2+}, Ca^{2+}, Sr^{2+}, and Ba^{2+} choride solutions, J. Colloid Interf. Sci. 97 (1984) 446–455.
[25] R.M. Pashley, The effects of hydrated cation adsorption on surface forces between mica crystals and its relevance to colloidal systems, Chem. Scripta 25 (1985) 22–27.
[26] J.P. Guilloteau, M.M. Rieskautt, A.F. Ducruix, Variation of lysozyme solubility as a function of temperature in the presence of organic and inorganic salts, J. Cryst.Growth 122 (1992) 223–230.
[27] T. Aarakawa, R. Bhat, S.N. Timasheff, Preferential interactions determine protein solubility in 3-component solution, the $MgCl_2$ system, Biochemistry 29 (1990) 1914–1923.
[28] R.A. Curtis, J.M. Prausnitz, H.W. Blanch, Protein-protein and protein-salt interactions in aqueous protein solutions containing concentrated electrolytes, Biotechnol. Bioeng. 57 (1998) 11–21.
[29] D.E. Kuehner, H.W. Blanch, J.M. Prausnitz, Salt-induced protein precipitation: phase equilibria from an equation of state, Fluid Phase Equilibr. 116 (1996) 140–147.
[30] G.A. Krestov, Thermodynamics of Solvation: Solution and Dissolutions, Ions and Solvents, Structure and Energetics, Horwood, New York, 1991.
[31] O.Y. Samoilov, in: R.A. Horne (Ed.), Water and Aqueous Solutions: Structure, Thermodynamics, and Transport Processes, Wiler-Interscience, New York, 1972, pp. 597–612.
[32] D.E. Kuehner, J. Engmann, F. Fergg, M. Wernick, H.W. Blanch, J.M. Prausnitz, Lysozyme net charge and ion binding in concentrated aqueous electrolyte solutions, J. Phys. Chem. B 103 (1999) 1368–1374.
[33] P. Retailleau, M. Ries-Kautt, A. Ducruix, No salting-in of lysozyme chloride observed at low ionic strength over a large range of pH, Biophys. J. 72 (1997) 2156–2163.
[34] M. Ries-Kautt, A. Ducruix, Inferences drawn from physicochemical studies of crystallogenisis and precrystalline state, Methods Enzymol. 276 (1997) 23–59.